INFLUENCE OF PIEZO-ACTIVE ACOUSTIC VIBRATIONS ON CHARGE TRANSPORT AND PHOTOLUMINESCENCE IN DOPED GaAs/AlGaAs STRUCTURES[1]

V.V. KURYLYUK, O.I. POLOVINA, O.A. KOROTCHENKOV

Taras Shevchenko Kyiv National University
(6, Academician Glushkov Ave., Kyiv 03127, Ukraine; e-mail: kuryluk@univ.kiev.ua)

UDC

Charge transfer processes in the two-dimensional electron gas of GaAs/AlGaAs hybrid structures subjected to piezo-active vibrations within ultrasound frequency range have been studied both experimentally and theoretically. Changes in the photoluminescence spectrum of such structures and the spatial variations of this spectrum in the excited high-frequency piezoelectric field have been registered experimentally. The data obtained are in good agreement with the results of numerical simulation. The piezoelectric field component normal to the GaAs-plane has been shown to control the processes of perpendicular charge transport in the structure concerned. A bend in the current-voltage characteristic of the structure, typical of the process of charge-carrier resonant tunneling through the barrier layer, has been registered; the corresponding model of band bending in the piezoelectric field has been proposed.

1. Introduction

The problem of charge transport in two-dimensional structures subjected to periodic loading invokes a hot interest and is a subject of a plenty of modern researches [1–4]. The purpose of this work is to make a comparative study, both experimental and theoretical, of charge transfer processes occurring in the two-dimensional electron gas (2DEG) of the GaAs/AlGaAs structure, where piezo-active acoustic vibrations (PAVs) are excited. The experimentally registered variations in the photoluminescence (PL) spectrum of this structure in the GaAs-layer plane, which take place owing to the action of the piezoelectric field, agree well with corresponding changes obtained by the numerical simulation. The component of the piezoelectric field normal to the GaAs-plane is capable to affect the processes of perpendicular charge transport in the structure, which is evidenced by the studies of current-voltage characteristics (CVCs).

2. Research Technique

2.1. Experimental specimens

Specimens for studying were two-layer structures consisting of a piezoelectric transducer and a GaAs/AlGaAs semiconductor heterostructure (Fig. 1). In experiments, heterostructures of two types were used, which differed in the dimensions of their GaAs quantum wells (QWs). In the structures of type I, a multilayered doped structure with 20 periods of GaAs quantum wells, each of the thickness $L_W = 6.1$ nm, separated by $Al_{0.5}Ga_{0.5}As$ barrier layers 50 nm in thickness each, was grown up (Fig. 2). In the structures of type II, 30 periods of GaAs quantum wells of the thickness $L_W = 10$ nm each were separated by the $Al_{0.5}Ga_{0.5}As$ barrier layers with the same thickness.

While studying PL, optically polished $LiNbO_3$ wafers of the 128°-Y- rotated cut with the linear dimensions $L_X \times L_Y \times L_Z = 13.8 \times 0.785 \times 3.75$ mm^3 were used as a source of piezoelectric fields. For the excitation of PAVs in the researched specimens, metal electrodes were deposited onto the opposite xz-faces of the $LiNbO_3$ wafers, and the high-frequency (HF) voltage $V_{\mathrm{HF}} = V_0 e^{i\omega t}$ was applied to them (Fig. 1,a). Researches were carried out at the resonance frequencies (the excitation frequencies of characteristic vibrations) of the specimen $\omega_{r,n}$ (n is an integer). The results of our theoretical calculations and experimental measurements testified that, provided this scheme of excitation, the characteristic vibrations of $LiNbO_3$ wafers are overtones of mode No. 8 ("dilation") in the Holland system of notations [5]. Experimentally, the frequencies $\omega_{r,n}$ were determined following the standard way – by the positions of maxima in the frequency dependence of the total conductivity of the $LiNbO_3$ wafer [6]. Within the studied frequency range $\omega/(2\pi)$ (from 0.2 to 1.3 MHz), seven overtones of this mode became excited ($n = 1 \div 7$).

[1]The results of the work were reported at the 3-rd Ukrainian Scientific Conference on Semiconductor Physics (June 17–22 2007, Odessa, Ukraine).

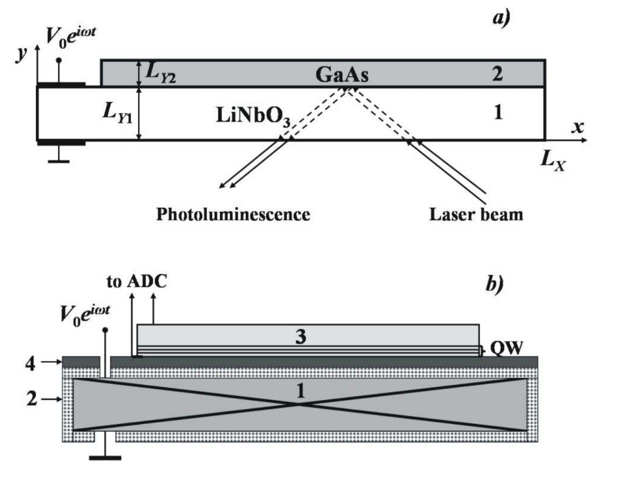

Fig. 1. *a* – combined cell "piezoelectric ($LiNbO_3$, *1*)–semiconductor (GaAs, *2*)"; $V_0e^{i\omega t}$ is the exciting high-frequency voltage with the frequency ω. *b* – combined cell for the measurements of current-voltage characteristics: *1* – piezoelectric ceramics, *2* – metallic screen, *3* – GaAs/AlGaAs structure, *4* – dielectric layer, QWs are GaAs quantum wells

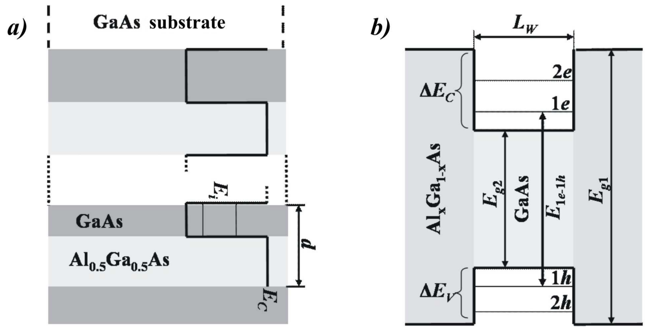

Fig. 2. Fragment of researched structures with GaAs quantum wells (*a*) and the corresponding energy band structure (*b*). E_C approximates the profile of the conduction-band bottom normally to the structure layers. The profile forms a barrier for electrons in the $Al_xGa_{1-x}As$ layer; the barrier height is $\Delta E_C = 1.1x$ at $0 \le x \le 0.45$ and $\Delta E_C = 0.43 + 0.14x$ at $0.45 < x \le 1$ [7]. The levels E_i mark the calculated electron energy states in the QW

Elastic and piezoelectric fields, which arise when PAVs are excited in the $LiNbO_3$ wafer, propagate beyond the boundaries of the latter and penetrate into the semiconductor structure, which is in contact with the wafer. In so doing, if the heterostructure dimensions are as was indicated above, no standing waves appear in the specimen at frequencies $\omega_{r,n}$, i.e. the entire specimen vibrates as a whole. In addition, since the layers with QWs are located at a distance of approximately from 30 to 1120 nm from the heterostructure-I surface and the surface of the $LiNbO_3$ wafer is optically polished, it is possible to assume that the spatial distributions of the piezoelectric field strength components in the semiconductor structure are identical to those on the $LiNbO_3$-wafer surface.

2.2. Photoluminescence researches

Low-temperature (6 K) PL was excited in specimens by laser light with the quantum energy $h\nu \approx 1.9$ eV (the 647.1-nm line of a Kr^+-laser) and the irradiation power $P \approx 10$ W/cm^2. The quantum energy of exciting light, $h\nu$, exceeded the energy of exciton ground state in GaAs wells ($E_{1e-1h} = 1.603$ eV in Fig. 2,*b*), but was smaller than the energy gap width of barrier layers ($E_{g1} = 2.095$ eV in Fig. 2,*b*). The positions of energy levels of electrons, E_{ie}, and holes, E_{ih}, in QWs were determined on the basis of calculations made for the dependence of the transmission factor D on the energy E of charge carriers in the case of a model structure confined by the emitter and a GaAs quantum well with two AlGaAs barriers. In this case, the energy barrier is equal to ΔE_C for electrons and $\Delta E_V = \Delta E_g - \Delta E_C$ for holes, where ΔE_g is the difference between the energy gap widths in the barrier ($Al_xGa_{1-x}As$) and well (GaAs) materials [6],

$$\Delta E_g = E_{g1} - E_{g2} = 1.425 + 1.15x + 0.37x^2 - E_{g2}. \quad (1)$$

The effective masses of electrons and holes in the barrier region were determined by the relations $m_e^* = 0.067 + 0.083x$ and $m_h^* = 0.087 + 0.063x$, respectively [7]. The sections in the obtained dependences $D(E)$, where the coefficient D grew drastically, were used to determine the resonance energy E_i for electrons and holes, which corresponded to the energy positions of levels in the QWs of the structure under investigation (Fig. 2). The energies E_{ie} of the electron levels were equal to 54 and 205 meV in the case of the type-I structures, and to 38, 150, and 325 meV for the structures of type II. The corresponding states E_{ih} for holes were characterized by the energies 39 and 137 meV in the structures of type I and 19, 74, and 151 meV in the structures of type II.

Taking the values for the coefficients of light absorption and reflection as $\alpha = 2 \times 10^4$ cm^{-1} and $R = 0.3$, respectively [8], we determine the energy $\Delta I = \left(1 - e^{-\alpha d}\right)(1 - R)\,P \approx 0.09$ J/(s $\times$ cm^2), which is absorbed by a unit area of the QW interlayer within a unit time interval. Then, the two-dimensional density

n_{2D} of photoinduced charge carriers can be evaluated as

$$n_{2\mathrm{D}} = \frac{\Delta I}{h\nu}\,\tau, \qquad (2)$$

where τ is the lifetime of an electron-hole pair in the well. For $\tau = 1$ ns [9], we obtain $n_{2D} \approx 3\times10^8$ cm^{-2}. Between the structure and the substrate, a doped GaAs:Si layer, which ensured the density of 2DEG in the QW to be of about 10^{11} cm^{-2}, was grown up. PL was registered with time resolution which allowed the moment of registration to be shifted with respect to the start of exciting signal. The data reported below, which concern the redistribution of charge carriers in the QW plane, were obtained in a specimen with the type-I structure.

2.3. CVCs measurements

Data concerning the charge transport in the direction perpendicular to QW layers were obtained making use of heterostructures of type II. In this case, the CVC variations caused by the PAV excitation in the structures were registered.

For CVC measurements, a cell presented in Fig. 1,*b* was used. In–Ga contacts were deposited onto the opposite sides of the heterostructure; the contact dimensions were 4×4 mm^2 on the substrate side and 2×2 mm^2 on the structure surface. To exclude the influence of electric stray fields generating by the exciting HF voltage V_{HF} on the input circuits of the equipment, piezoceramic transducer *1* used to excite PAVs was surrounded by metal foil screen *2*, and studied heterostructure *3* was pressed to this screen. The piezoelectric transducer was supplied with the voltage V_{HF} generated by an external G3-41 HF-generator. Between the heterostructure and the piezoelectric transducer, thin dielectric layer *4* was placed in order to prevent the electric coupling between the circles of direct (CVC measurements) and alternative (PAV excitation) currents, but not to interfere the acoustic coupling between the piezoelectric transducer and the heterostructure.

Therefore, in our experiments, the piezoelectric fields emerged in the researched heterostructure owing to its own piezoelectric effect. CVCs were registered in the automatic mode with the help of a computer-assisted installation created on the basis of an ADA-1292 analog-to-digital converter. The CVCs described below were registered at a temperature of 77 K.

2.4. Calculation of piezoelectric fields and simulation of charge transfer processes

Earlier, in work [10], the procedure of calculation of resonance (characteristic) frequencies and three-dimensional spatial distributions of elastic displacement and piezoelectric strength fields at those frequencies making use of the Rayleigh–Ritz variational method has been expounded in detail for the case of PAVs in an isolated $LiNbO_3$ wafer. In this work, the method was extended onto the case of two-layer structure (Fig. 1,*a*). For this purpose, the functional H (see formula (9) in work [10]) was selected in the form $H = H_1 + H_2 + H_M + H_E$. Here, the summands H_1 and H_2, which describe layers 1 and 2, are written down in the form proposed earlier by Holland and Eer Nisse [5, 11]. For the summands H_M and H_E, which describe acoustic and electric boundary conditions at the interface S_h, the following expressions were used:
in the case of a "sticking" contact,

$$H_M = \iint\limits_{S_h} N_j (U_{(2)i} - U_{(1)i}) T_{(1)ij} dS \qquad (3)$$

in the case of a "slippery" contact,

$$H_M = \iint\limits_{S_h} N_j (U_{(2)j} - U_{(1)j}) T_{(1)jj} dS \qquad (4)$$

and, for any acoustic contact,

$$H_E = \iint\limits_{S_h} N_m (\Phi_{(2)} - \Phi_{(1)}) D_{(1)m} dS \qquad (5)$$

where $\vec{U} = \{\vec{U}_{(1)}, \vec{U}_{(2)}\}$ is the elastic displacement vector, $\Phi = \left\{\Phi_{(1)}, \Phi_{(2)}\right\}$ the piezoelectric potential, and subscripts 1 and 2 correspond to layers 1 and 2, respectively (Fig. 1,*a*).

The calculation of the piezoelectric fields $\vec{E} = \left\{-\vec{\nabla}\Phi_{(1)}, -\vec{\nabla}\Phi_{(2)}\right\}$ in a two-layer structure depicted in Fig. 1,*b* can be carried out by considering the acoustic contact between layers as sliding and making use of boundary conditions (4). Since the piezoelectric transducer and the heterostructure are electrically decoupled, the term $H_E = 0$. Numerical calculations demonstrates that, at the amplitude $V_0 = 50$ V which was used in our experiments, the maximal strength of intrinsic piezoelectric fields in heterostructures reached $10^4 \div 10^5$ V/cm depending on the frequency.

Numerically calculated distributions of the piezoelectric potential Φ at the resonance frequencies

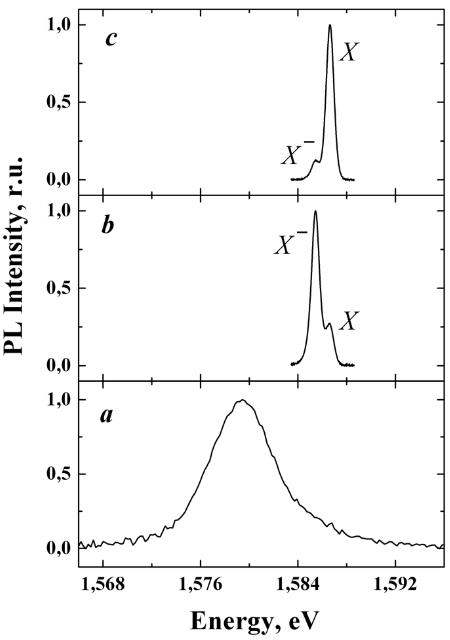

Fig. 3. PL spectra of the GaAs/AlGaAs structure (type I) registered at different surface points (see Fig. 4) at the same time moment with respect to the application of HF voltage

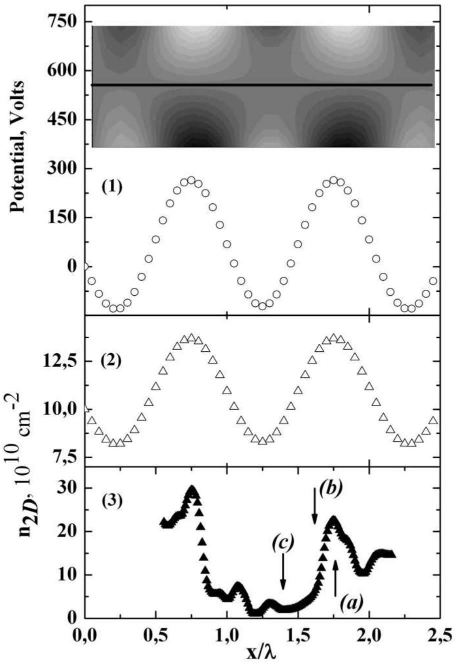

Fig. 4. (*1*) – calculated distribution of the piezoelectric potential in the middle ($z = L_Z/2$) xy-plane (the inset) in the geometry of Fig. 1,*a* and along the x-axis at the interface $LiNbO_3$ wafer–semiconductor structure (the horizontal line in an inset). Dark regions correspond to $\Phi < 0$, light ones to $\Phi > 0$. The calculated (*2*) and measured (*3*) redistributions of the 2DEG density in a piezoelectric field along the x-axis (the distance is reckoned in the wavelength λ units) in the QW plane located at the interface. The frequency amounts to 728 kHz for panels *1* and *2*, and 734 kHz for panel *3*. The applied HF voltage is 10 V for the calculations and 100 V for the dependence in panel *3*. Points (*a*) to (*c*) in panel *3* correspond to spectra (*a*) to (*c*) in Fig. 3

allowed a quantitative simulation of charge transfer processes in a GaAs specimen to be carried out and the corresponding spatial redistributions of the PL intensity and spectrum to be obtained. For the simulation, we used the standard equations describing diffusion and drift of charge carriers [12]. The equations were solved making use of the finite element method [13].

3. Results and Their Discussion

The emergence of the piezoelectric potential in the heterostructure (see Fig. 1,*a*) gives rise to a substantial redistribution of charge carriers in the QW plane. The PL spectrum of the studied structure (it is not shown in the figure) demonstrates a broad band of radiation emission, characteristic of the recombination between electrons belonging to the 2DEG and photoexcited holes. The radiation spectrum shape was found to change considerably with the variation of density in the 2DEG [14], which allows the variation of this quantity (n_{2D}) under the action of piezoelectric fields to be studied. Some of the results obtained are presented in Fig. 3.

If the piezoelectric potential is positive at a certain point ($\Phi > 0$, dark regions in Fig. 4(*1*)), the PL excitation broadens its radiation spectrum (Fig. 3,*a*). On the contrary, as the point of PL excitation moves into the region where $\Phi < 0$ (light regions in Fig. 4(*1*)), the radiation spectrum becomes substantially narrower; it becomes shifted towards the blue spectral range and starts to reveal the lines of neutral (X) and negatively charged (X^-) excitons (panels *b* and *c*, respectively, in Fig. 3). It was found earlier [14] that such an evolution of the spectrum originates from the variation of electron density in the 2DEG under the application of an external electric field. It allows one to draw a conclusion that, being subjected to the action of a piezoelectric field, the electron density in the structure concerned becomes redistributed in the QW plane: it increases in those regions, where $\Phi > 0$, and, accordingly, decreases if $\Phi < 0$. This result is clear from the qualitative point of view, because electrons in the 2DEG are accumulated into the ($\Phi > 0$)-regions and pushed away from the

($\Phi < 0$)-ones. As a result, the charge carriers, being photoexcited in the region with the elevated density of the 2DEG, form – at recombination – a broadband radiation emission (see spectrum a in Fig. 3). On the contrary, radiative recombination in the region with a reduced 2DEG density gives rise to the narrow-band luminescence (spectra b and c in Fig. 3).

A more detailed study of the PL-spectrum shape makes it possible to determine numerical values for the n_{2D} density at various Φ-values. Really, in the case of PL in the 2DEG [15],

$$n_{\rm 2D} = \frac{\Gamma m_e}{\pi \hbar^2}, \tag{6}$$

while, for excitonic PL [16],

$$n_{\rm 2D} = \frac{m_e kT}{\pi \hbar^2} \ln\left(1 + \frac{I_{X^-}}{I_X} e^{E_b/kT}\right), \tag{7}$$

where Γ is the linewidth of the radiation emission from 2DEG (spectrum a in Fig. 3), I_{X^-} and I_X are the intensities of the corresponding exciton lines, and E_b is the energy distance between the X^-- and X-lines.

The analysis of the evolution of the PL spectrum shape, when the point of PL excitation becomes shifted at a fixed time moment, allowed us to determine the distribution of the 2DEG density in the QW plane; in Fig. 4, it is presented in the form of a dependence on the coordinate x. One can see that the maxima of the dependence $n_{\rm 2D}(x)$ correspond to the maxima of the calculated piezoelectric potential distribution $\Phi_2(x)$. The experimental data testify also to a capability of rather an efficient control over the 2DEG density in the QW plane by means of a piezoelectric field, with the formation of depleted 2DEG regions (the minima in Fig. 4(*3*)).

Making use of a structure with double QWs separated by a thin $Al_{0.2}Ga_{0.8}As$ barrier layer with a reduced barrier height (cf. 500 meV for $Al_{0.5}Ga_{0.5}As$ and 220 meV for $Al_{0.2}Ga_{0.8}As$) allowed us to register a transition to indirect PL with the recombination of electrons and holes localized in neighboring QWs [4]. The transition occurs, if the growth of the normal F_y-component of the piezoelectric field is accompanied by the growth of the voltage $V_{\rm HF}$. In this work, the contribution of the field component F_y to the processes of perpendicular charge transport is illustrated by the results of our researches dealing with the CVCs of type-II structures.

Excitation of PAVs gives rise to the increase of the current through the structure (Fig. 5) and to the appearance of a characteristic bend in the vicinity of $V = 1$ V (the arrow in Fig. 5,c). Taking into account the mechanisms of charge transfer in cascade systems with QWs [17, 18], the indicated current growth can be explained by the overbarrier excitation of charge carriers subjected to the action of PAVs, and the CVC bend by the processes of tunnel charge transport [19, 20]. The

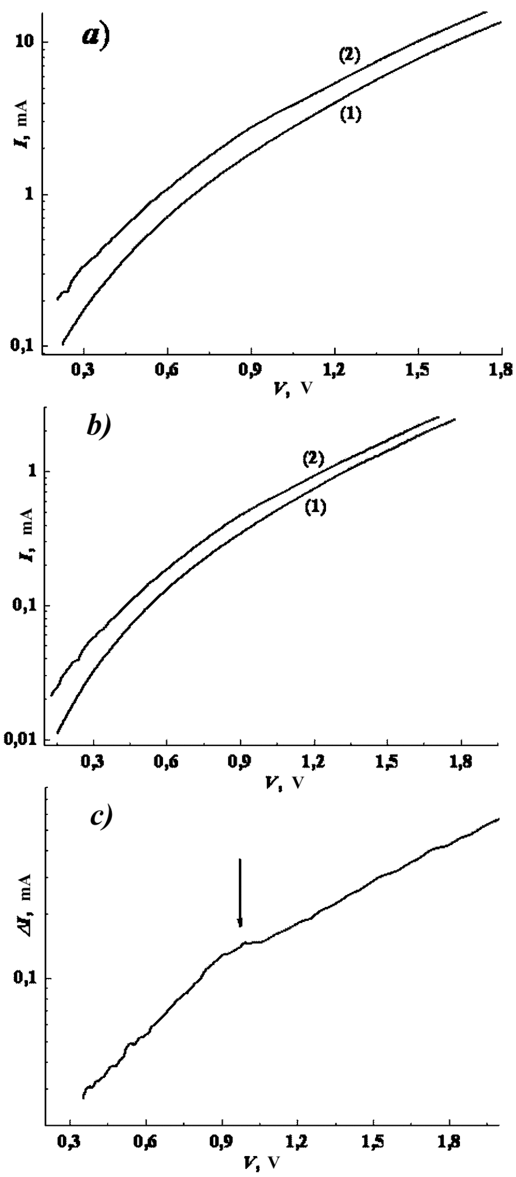

Fig. 5. Forward (a) and reverse (b) current-voltage characteristics of the type-II structures in the absence (*1*) and under the action of PAVs (*2*). (c) Variation ΔI of the current through the structure as a function of the applied voltage V under the action of PAVs stimulated by the 50-V HF voltage with a frequency of 225 kHz

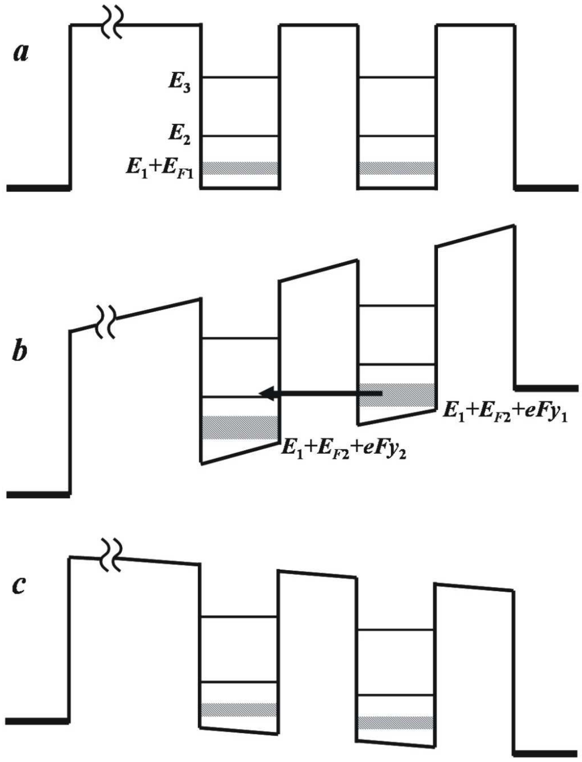

Fig. 6. Model of resonant tunneling through the GaAs/AlGaAs structure (type II): band structure in the absence of voltage V (panel a) and for a non-zero applied voltage and the vibration excitation at different half-cycles of the applied HF field (panels b and c). The arrow corresponds to the resonant tunneling of an electron. The transformation of bands in panel b into narrow energy levels in panel c illustrates the reduction of $n_{\rm 2D}$ owing to the processes of charge transfer in the QW planes

latter phenomenon has to manifest itself at transitions of electrons from the emitter to the collector (from the substrate to the near-surface layer or vice versa, depending on the V-polarity) making use of the QW energy levels, provided that the electron energies on the left- and right-hand sides of the barrier are identical (resonant tunneling).

The model of resonant charge transfer in the structure concerned is illustrated in Fig. 6. In the approximation of a degenerate 2DEG, the position of the Fermi level $E_{\rm F}$ can be determined – knowing the electron gas density – by the formula [21]

$$E_{\rm F} = E_1 + \frac{\pi\hbar^2 n_{\rm 2D}}{m_e^*}. \tag{8}$$

In the absence of applied fields, taking $n_{\rm 2D} \approx 10^{11}$ cm^{-2}, we obtain $E_{\rm F1} \approx E_1 + 3$ meV (Fig. 6,a). By substituting the value $n_{\rm 2D} \approx 3 \times 10^{11}$ cm^{-2} taken in the maximum (Fig. 4(3)), the position of the level in the presence of PAVs is evaluated as $E_{\rm F2} \approx E_1 + 10$ meV (Fig. 6,b). The edges of the conduction band become bent in the applied external field with the strength $F = F_V + F_{\rm HF}$, where F_V is the static and $F_{\rm HF}$ the HF oscillating field. Neglecting the inhomogeneity in the distribution of F_V inside the specimen and supposing that the external voltage V = 1 V is completely drops across the multilayered structure "barrier–QW", the estimation gives $F_V \approx 2 \times 10^4$ V/cm. At the same time, under the conditions of obtaining the results depicted in Fig. 5, the peak value is $F_V \approx 3 \times 10^4$ V/cm. Since $F_V < F_{\rm HF}$, the band bending within different half-cycles of the HF-field variation looks like those exhibited in Figs. 6,b and c.

Then, the condition of resonant electron tunneling following the scheme shown in Fig. 6,b is

$$E_2 - E_{\rm F2} = eFd. \tag{9}$$

Substituting the values $F = 5\times10^4$ V/cm and $d = 20$ nm (Fig. 2,a), we obtain $eFd = 100$ meV. Since $E_2 - E_{\rm F2} \approx$ 102 meV, relation (9) is valid indeed, which confirms that resonant tunneling is possible. Notice that the condition for the 2DEG enrichment with the maximal value $E_{\rm F2}$ is obeyed only in a confined region of the structure (Fig. 4(3)); at the same time, the capability of spatial and temporal resolution of the $I(V)$-dependence was not applied in these experiments. In this case, the maximal value of the expression on the left-hand side of Eq. (9) at the minimal value of $n_{\rm 2D}$ reaches $E_2 - E_1 =$ 112 meV, or 1.12 V in the units of voltage V (see Fig. 5). Hence, the condition of tunneling is fulfilled in a certain V-range, depending on the density $n_{\rm 2D}$ variation. One may assume that just this circumstance is responsible for the CVC bend in Fig. 5,c, instead of a resolved current jump, which is, in general, characteristic of tunnel processes [19, 20].

It is worth noting that the variation in the positions of the charge carrier energy levels in the QWs can be induced by the influence of a deformation as well. The magnitude of this variation $\Delta E_{\rm DP}$ can be estimated by the relation

$$\Delta E_{\rm DP} = D_{ik} U_{ik}, \tag{10}$$

where D_{ik} and U_{ik} are the components of the deformation potential and strain tensors, respectively. Since $D_{ik} \sim 1$ eV for GaAs [7] and the estimations give the maximal value of about 10^{-4} for deformations in our experiments, we obtain $\Delta E_{\rm DP} \approx 0.1$ meV. The value obtained for $\Delta E_{\rm DP}$ does not satisfy condition (9), which confirms our assumption about the influence of just piezoelectric fields on the processes of perpendicular charge transfer.

4. Conclusions

Comparative experimental and theoretical researches of the charge transfer processes in the two-dimensional electron gas of a GaAs/AlGaAs structure placed into a piezoelectric field of acoustic vibrations with ultrasonic frequency have been fulfilled. It has been demonstrated that the piezoelectric fields generated in the piezoelectric make it possible to efficiently control the spatial distribution of charge carriers in a two-layer system "piezoelectric–semiconductor heterostructure". The experimentally registered modifications of the PL spectrum produced by GaAs/AlGaAs quantum wells in the piezoelectric field are in good agreement with those obtained in the framework of the numerical simulation method. The component of the piezoelectric field, which is normal to the GaAs quantum well plane, was demonstrated to be capable of influencing the processes of perpendicular charge transfer in the structure, which has been confirmed by our researches of the current-voltage characteristics. A model has been proposed for the resonant tunneling through the GaAs/AlGaAs structure, which is induced by the bending of energy bands in the piezoelectric field.

The authors express their gratitude to O.Ya. Olikh for his help in the measurements of current-voltage characteristics.

1. T. Müller, A. Würtz, A. Lorke *et al.*, Appl. Phys. Lett. **87**, 042104 (2005).
2. J. Ebbecke, N.E. Fletcher, T.J. Janssen *et al.*, Appl. Phys. Lett. **84**, 4319 (2004).
3. M. Rotter, A.V. Kalameitsev, A.O. Govorov *et al.*, Phys. Rev. Lett. **82**, 2171 (1999).
4. O.A. Korotchenkov and A. Cantarero, Phys. Rev. B **75**, 0853201 (2007).
5. R. Holland, J. Acoust. Soc. Amer. **43**, 988 (1968).
6. *Physical Acoustics. Principles and Methods*, edited by W.P. Mason (Academic Press, New York, 1964), Vol. 1A.
7. S. Adachi, *Physical Properties of III – V Semiconductor Compounds* (Wiley, New York, 1992).
8. W. Wegscheider, L.N. Pfeiffer, M.M. Dignam *et al.*, Phys. Rev. Lett. **71**, 4071 (1993).
9. J. Feldmann, G. Peter, E.O. Gobel *et al.*, Phys. Rev. Lett. **59**, 2337 (1987).
10. O.I. Polovina, V.V. Kurylyuk, and O.O. Korotchenkov, Ukr. Fiz. Zh. **58**, 230 (2007).
11. R. Holland and E.P. Eer Nisse, IEEE Trans. Sonics and Ultrasonics **15**, 119 (1968).
12. V.L. Bonch-Bruevich and S.G. Kalashnikov, *Physics of Semiconductors* (Nauka, Moscow, 1977) (in Russian).
13. O.C. Zienkiewicz, *The Finite Element Method in Engineering Science* (McGraw-Hill, Maidenhead, 1971).
14. G. Finkelstein, H. Shtrikman, and I. Bar-Joseph, Phys. Rev. Lett. **74**, 976 (1995).
15. R. Rapaport, G. Chen, D. Snoke *et al.*, Phys. Rev. Lett. **92**, 1174051 (2004).
16. A. Manassen, E. Cohen, A. Ron *et al.*, Phys. Rev. B **54**, 10609 (1996).
17. N. Peyghambarian, S.W. Koch, and A. Mysyrowicz, *Introduction to Semiconductor Optics* (Prentice Hall, Englewood Cliffs, 1993).
18. C. Gmachl, F. Capasso, D.L. Sivco *et al.*, Rep. Prog. Phys. **64**, 533 (2001).
19. S. Tarucha and K. Ploog, Phys. Rev. B **39**, 5353 (1989).
20. T. Ohtsuka, L. Schrottke, R. Hey *et al.*, J. Appl. Phys. **94**, 2192 (2003).
21. A.Ya. Shik, L.G. Bakueva, and S.F. Musikhin, *Physics of Low-Dimensional Systems* (Nauka, St. Petersburg, 2001) (in Russian).

Received 25.10.07.
Translated from Ukrainian by O.I. Voitenko

ВПЛИВ П'ЄЗОАКТИВНИХ АКУСТИЧНИХ КОЛИВАНЬ НА ПРОЦЕСИ ПЕРЕНЕСЕННЯ ЗАРЯДУ ТА ФОТОЛЮМІНЕСЦЕНЦІЮ В ЛЕГОВАНИХ СТРУКТУРАХ GaAs/AlGaAs

В.В. Курилюк, О.І. Половина, О.О. Коротченков

Р е з ю м е

Проведено порівняльні експериментальні й теоретичні дослідження процесів перенесення заряду у двовимірному електронному газі в структурі GaAs/AlGaAs під дією п'єзоактивних акустичних коливань (ПАК) ультразвукової частоти. Експериментально зареєстровано зміни спектра фотолюмінесценції (ФЛ) та її просторового розподілу в збуджувальному високочастотному п'єзоелектричному полі. Наведені дані добре узгоджуються зі змінами, отриманими чисельним моделюванням. Показано, що нормальна до площини GaAs складова п'єзоелектричного поля здатна впливати на процеси перпендикулярного перенесення заряду у структурі. Зареєстровано перегин на вольт-амперній характеристиці структури, характерний для резонансного тунелювання крізь бар'єрні шари, і запропоновано відповідну модель вигину зон у п'єзоелектричному полі.